REVIEW ARTICLE

Narrowband photon pair generation and waveform reshaping

J. F. Chen[1,*], **Shengwang Du**[2,†]

[1] *Department of Physics, East China Normal University, Shanghai 200241, China*

[2] *Department of Physics, The Hong Kong University of Science and Technology, Clear Water Bay, Kowloon, Hong Kong, China*

*E-mail: *jfchen@phy.ecnu.edu.cn, †dusw@ust.hk*

In this article, we review on narrowband photon pairs produced in nonlinear crystals, and especially in atomic ensembles. In atomic ensembles, "write–read" process in pulse mode and spontaneous four-wave mixing process (SFWM) in continuous mode are two popular photon pair generation schemes. We specifically discuss the experimental works with continuous SFWM scheme in cold atomic ensembles. Photon pairs produced in these systems are characteristic of controllable long coherence time, and therefore are accessible with direct temporal modulation. We elaborate on the recent techniques on modulation and waveform reshaping of narrow-band paired photons.

Contents

1 Introduction

1.1 History and motivation

Photon pairs with nonclassical correlation find wide application in quantum information processing, quantum computation, quantum cryptography, quantum imaging, and other quantum optics related areas [1–3]. There are some early works on photon pair generation in atomic medium, through positronium annihilation [4], or atomic cascade [5, 6]. Following the fast developing laser technology and nonlinear optics, paired photons are easily produced from spontaneous parametric down conversion (SPDC) with nonlinear crystal in 1960's [7, 8]. For decades, SPDC become a standard method to generate paired photons and the optical properties of SPDC paired photons have been well studied [9–11]. However, the SPDC paired photons suffer from limitations for certain applications: broad linewidth ($\sim$ THz) and low spectral brightness; coherence time in the sub-picosecond range, which is not resolvable by existing photodetectors; short coherence length (~ 100 μm) which puts difficulty on long distance quantum communication. Various techniques developed to lengthen the generated paired photons. By using nonlinear crystal and cavities, paired photons with linewidths of about 10 MHz and correlation times of about 50 ns are obtained [12–17]. The correlation time therefore is determined by the external cavity, and is not controllable.

Duan's proposal of long-distance quantum communication described a scheme that allows the implementation of quantum communication with high fidelity over long distance among atomic ensembles [18]. The idea of storing photonic states into atomic spin states therefore motivated the search for methods for generating narrowband correlated photons in atomic ensembles. Lukin [19] and Kimble's group [20] almost simultaneously reported the experimental demonstration of correlated paired pho-

ton. When induced by a write pulse, atomic spin excitations are produced via spontaneous Raman transition with Stokes photons and corresponding flipped atomic spin states are created. The stored spin wave can be retrieved with a read pulse (or called retrieve pulse), so the atomic spin states produce the anti-Stokes photons via a second Raman transition. The generated paired photons involving atomic spin states storing and retrieving are shown to be highly correlated. Kuzmich *et al.* [20] also showed the nonclassical correlations of the generated photon pair by demonstration of the violation of Cauchy-Schwartz inequality. In such a "write–read" procedure, the paired photons are not maximally time-frequency entangled because the writing and reading happen in separate processes. To solve this problem, four-wave mixing process with both controlling beams present in a generation cycle are developed. Balić *et al.* [21] used a 3D magneto–optical trap to generate paired photons with controllable waveform; Kolchin *et al.* [22] developed a configuration where a single laser served as the pump and coupling driving fields simultaneously; Du *et al.* [28] demonstrated paired photons generation in a two-level atomic system. In their configuration, the photon pairs are time–frequency entangled [23, 24]. With 2D MOT, Du *et al.* [25] generated narrow-band paired photon in medium with high optical depth. The coherence time of the paired photons is approaching 1 μs and controllable via slow light effect.

One of the main goal for this article is to review the recent development of paired photons generated in atomic ensembles. Especially, latest works of paired photons generation in cold atom ensembles, employing laser cooling [28–32] and electromagnetically-induced transparency [33, 34], make the near- and on-resonance nonlinear processes efficient. Laser cooling and trapping of neutral atoms cools down atoms to about 100 μK or below, and therefore Doppler broadening can be neglected. For rubidium 85, for example, natural broadening of atomic excited states generates atomic decay rate as small as $2\pi \times 6$ MHz for rubidium atoms 5P states (orbital momentum $l = 1$), and therefore the lifetime of 5P excited states could be as long as 27 ns [35, 36]. The reduced decay rate is a significant factor to make the paired photon waveform measurable with present commercial photodetector. Also, narrow linewidth enable atoms to interact with resonant light efficiently and facilitate nonlinear interactions. On the other hand, electromagnetically-induced transparency (EIT) eliminates absorption on resonance and enhances nonlinear interactions at low light level [37, 38]. The other main section investigates the paired photon waveform reshaping issues, covering experimental approaches both in SPDC and atomic ensembles. We review in detail the recent works on temporal waveform reshaping of paired photons with electro–optical modulator, which are po-

tential schemes for nonclassical light source manipulation used in quantum communication.

1.2 Correlated and entangled paired photons

Paired photons exhibit correlation, either classical or nonclassical. There were several attempts to produce correlated photons from room-temperature atoms as early as 1980s [39–42]. The schemes are based on a right-angle pump configuration for photons generation in two-state atoms. But the uncorrelated count rate caused by the strong Rayleigh scatter of the pump laser diminished the nonclassical feature, i.e., the Cauchy–Schwartz inequality is not violated. For a classical light source, the cross correlation of the paired photons is limited by the product of their auto-correlations: $[g^{(2)}_{s,as}(\tau)]/(g^{(2)}_{s,s} g^{(2)}_{as,as}) \leqslant 1$. Therefore, violation of Cauchy–Schwartz inequality indicates nonclassical correlation.

Entangled paired photons, or termed as biphoton, are a special group of correlated paired photons. The two-photon state cannot be expressed as the product of the sub-state of each photon. Entanglement is one of the most surprising consequences of quantum mechanics, which seems to totally break our classical view over the physical world. The foundation of quantum mechanics has been a hot topic of debate for many years, including the famous statement made by Einstein, Podolsky, and Rosen [43] in 1935. At the same time, they raised a classic example for a two-particle entangled state:

$$|\psi\rangle = \sum_{a,b} \delta(a + b - c_0)|a\rangle|b\rangle \qquad (1)$$

where a and b are the momentum or the position of particle 1 and 2, respectively. The δ function indicates the absolute correlation between two particles.

Another example of entangled two-particle system can be well demonstrated by the EPR-Bohm entangled states. Suppose the polarization of either photon (marked by 1 and 2 respectively) is written as: $|\psi\rangle_{1(2)} = H_{1(2)}|H\rangle + V_{1(2)}|V\rangle$, where H,V represents horizontally, vertically polarized state respectively. The product state gives $H_1 H_2 |HH\rangle + H_1 V_2 |HV\rangle + H_2 V_1 |VH\rangle + V_1 V_2 |VV\rangle$. Explicitly, EPR-Bohm entangled states

$$|\psi\rangle_{\text{Bohm}} = \frac{1}{\sqrt{2}}(|HV\rangle \pm |VH\rangle) \qquad (2)$$

Clearly, Eq. (2) is different from the product state.

Bell's inequality [44] is violated by certain quantum mechanical statistical predictions. Later on the violation of Bell's inequalities become a standard of entangled states. The first edition of Bell's inequalities was not able to be tested directly by real experiments, until a refined edition was introduced by Clauser, Horne, Shimony and Holt [45]. Experimental works on time-frequency entan-

glement [21, 22, 28], momentum–position entanglement [46], polarization entanglement [16, 47, 48] have been reported.

1.3   Wide-band and narrowband paired photons source

Spontaneous parametric down conversion produces paired photons with bandwidth of THz, which are classified as wide-band paired photons, with extremely short coherence time. By applying a strong pump laser on a type of noncentrosymmetric crystal, the input pump photon annihilates and two down-converted photons termed signal and idler are created, with energy and momentum conservation preserved in the generation process. Consequently, SPDC paired photons are entangled in time–energy and position–momentum dimensions. Type-I and type-II SPDC processes are defined according to the polarization of the signal and idler photons generated in the parametric down conversion: In type-I SPDC, signal and idler are identically polarized (both ordinary or extraordinary); In type-II SPDC, they are orthogonally polarized (one is ordinary and the other is extraordinary). Following the perturbation theory described above, the two-photon amplitude of type-I SPDC is expressed as the form of [10]

$$\Psi(t_1, t_2) \sim e^{-\sigma_+^2 (t_1 + t_2)^2} e^{-\sigma_-^2 (t_1 - t_2)^2} e^{-i\bar{\omega}_s t_1} e^{-i\bar{\omega}_i t_2} \quad (3)$$

in which t_1, t_2 are the detection times for detector D_1 and D_2. ω_s, ω_i correspond to the central frequency for signal and idler, respectively. $1/\sigma_+$, $1/\sigma_-$ are characteristic coherence times that localize the two-photon wavepacket in $t_1 + t_2$ and $t_1 - t_2$ directions, respectively. In contrast, for type-II SPDC, the wave packet is unsymmetrical respect to the zero delay time ($\tau = t_1 - t_2$):

$$\Psi(t_1, t_2) \sim e^{-\sigma_+^2 (t_1 + t_2)^2} \Pi(t_1 - t_2) e^{-i\bar{\omega}_s t_1} e^{-i\bar{\omega}_i t_2} \quad (4)$$

The rectangular function is defined as $\Pi(t_1 - t_2) = 1$ for $0 \leqslant t_1 - t_2 \leqslant (L/v_o - L/v_e)$, and otherwise $\Pi(t_1 - t_2) = 0$. v_o, v_e corresponds to the group velocities for ordinary and extraordinary rays of the crystal respectively. As shown in Eq. (3) and Eq. (4), different from the symmetric wave packet for type-I SPDC, unsymmetrical rectangular shape is obtained in type-II SPDC.

In order to have EPR-Bohm type entangled polarization state, it is natural to use type-II SPDC, which produces orthogonal polarized photon pair. The signal idler pairs are emitted into two cones, one ordinary polarized and the other extraordinary polarized. With proper conditions the two cones can intersect, and along the intersection lines two-photon state is entangled with both space–time and polarization. However, type-II SPDC did not immediately show the EPR-Bohm entanglement in the early years as expected. Oppositely, polarization entanglement was demonstrated firstly in type-I SPDC, with the help of a beam splitter [49]. It took many

years for Shih [50] and Rubin [9] to realize the problem for type-II SPDC: With the "walk-off" problem, the two-photon wavepackets for polarization states, $o_1 e_2$ and $e_1 o_2$, are separate from each other in time, i.e., they become distinguishable by the click–click action of two detectors, since extraordinary polarized photons click the detector first. To obtain EPR-Bohm entangled states from these paired photons, the straightforward method is to compensate the delay time generated in the propagation, which was first demonstrated in experiment by Kwiat *et al.* [48]. Time–energy and position–momentum entanglement give rise to high dimensional entangled states which encode increasingly large amount of information, and therefore facilitate quantum information processing [51–53].

Considering the bandwidth of photon source, traditional SPDC produce wide-band paired photons. On one hand, wide-band paired photons are being pushed to ultrabroadband, with all the energy concentrate within a fs temporal range, to maximize the two photon probability transition [85]. On the other hand, to increase the short correlation time of SPDC paired photons, a high finesse optical cavity is utilized by Ou *et al.* to narrow down the linewidths [12]. In their work, the type-I parametric down converter inside the cavity produces paired photons with correlation time above 30 ns. They pointed out that the correlation time is inversely proportional to the bandwidth of down-conversion fields of the optical parametric oscillator. Also, the signal is enhanced by the resonance and the enhancement factor is given approximately by the square of the number of bounces of light in the cavity. Shi *et al.* recently give an experimental review on cavity enhanced SPDC [54]. The other related work is that, Chuu and Harris [55] suggested resonant backward-wave SPDC scheme, in which the gain linewidth for paired photons is reduced by a factor of 38 compared to forward-wave interaction.

Generation of paired photons is also developed in optical fiber, which is potential to be applied into communication. Parametric processes are firstly demonstrated in multi-mode fiber [56, 57], and later in single mode [58, 59]. There are rich literature on paired photons generation in optical fiber making use of $\chi^{(3)}$ nonlinearity [60–62].

2   Narrowband paired photons generation in atomic ensembles

2.1   "Write–read" process in pulse mode

Following DLCZ protocol [18], correlated paired photons are generated from ^{87}Rb vapor cell [19] and from Cs MOT [20]. With spontaneous Raman transitions, correlated pairs of Stokes photons and the optical state is

written into the atomic ensemble as flipped atomic spins. After a programmable time delay, the state stored in the spin wave is retrieved (or called "read") with a second Raman transition, and be converted to anti-Stokes fields, as shown in Fig. 1. The strong intensity correlation between the two beams implies that the fluctuation of the Stokes fields is mapped into the anti-Stokes fields. The photons pair from the "write" and "read" process violates Cauchy–Schwartz inequality due to nonclassical correlation between the generated fields. In this "write–read" process, the anti-Stokes photons are emitted with time delay controlled, and therefore the paired photons are not time–frequency entangled.
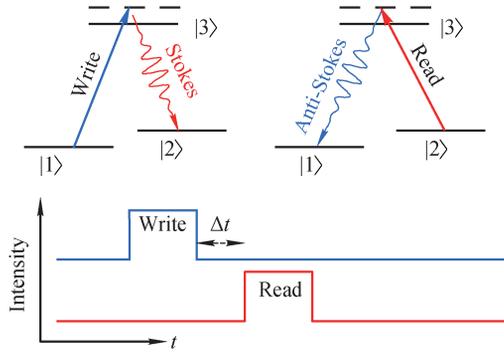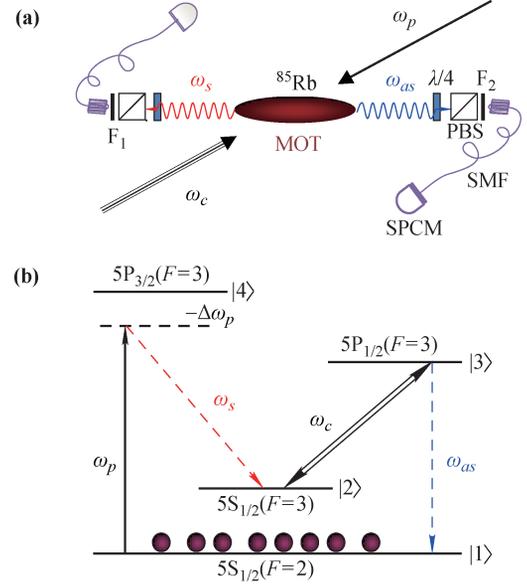

Fig. 1 Schematic of paired photons generation in write–read process with atomic ensemble.

2.2 Spontaneous four-wave mixing process (SFWM) in continuous mode

In this section we show in detail the continuous four-wave mixing process reported by Balić *et al.* [21] and Du *et al.* [25], and later by Lu *et al.* [26], and Chen *et al.* [27]. Paired photon waveform could be tuned with the help of EIT slow light effect. In the presence of counter-propagating, continuous pump (ω_p) and coupling beams (ω_c), phase matched Stokes (ω_s) and anti-Stokes (ω_{as}) photons are spontaneously generated in opposite directions, as shown in Fig. 2. The atomic ensemble is the two-dimensional ^{85}Rb magneto–optical trap with longitudinal length $L = 1.5$cm and temperature 100 μK. The atoms are all initially prepared in the ground state $5S_{1/2}$ $F = 2$. The pump and coupling beams are aligned at $2°$ from the longitudinal axis of the MOT, along which the paired photons are collected. Figure 2(b) shows the double-Λ energy level diagram, in which γ_{13} denote dephasing rates between $|3\rangle$ and $1\rangle$ and γ_{12} for two ground states.

Theoretical discussion on SFWM paired photons start from Heisenberg–Langevin equations or perturbation theory [75–77]. Three characteristic frequencies determine the paired photon waveform [78]: effective coupling Rabi frequency Ω_e; linewidth of the two resonances in nonlinear susceptibility $2\gamma_e$; full width at half-maximum phase-matched bandwidth $\Delta\omega_g = 2\pi \times 0.88/\tau_g$.

Fig. 2 Schematic of paired photons generation in four-wave mixing process with cold atomic ensemble, which is the same with Refs. [21, 25]. **(a)** Experimental configuration. **(b)** Double-Λ energy level diagram.

Competition of the three parameters defines the main feature of the waveform.

If $\text{Max}\{\Omega_e, \gamma_e\} < \Delta\omega_g$, the paired photon waveform exhibits Rabi oscillation. The longitudinal detuning function $\Phi(\omega)$ can be approximated as 1, and the two-photon amplitude is the Fourier transform of nonlinear parametric coupling coefficient $\kappa(\omega_{as})$. As indicated in Ref. [78], $\kappa(\omega_{as})$ is directly proportional to $\chi^{(3)}$, whose spectral function has two peaks with bandwidth $2\gamma_e$ and with peak separation Ω_e. Assuming that $\Omega_e = \sqrt{|\Omega_c|^2 - |\gamma_{13} - \gamma_{12}|^2} > 0$, the paired photon wavepacket is written as

$$\Psi(t_{as}, t_s) \simeq L\tilde{\kappa}(\tau)e^{-i(\omega_c+\omega_p)t_s}$$
$$= AE_pE_ce^{-\gamma_e\tau}[e^{-i(\bar{\omega}_{as}+\Omega_e/2)t_{as}}e^{-i(\bar{\omega}_s-\Omega_e/2)t_s}$$
$$-e^{-i(\bar{\omega}_{as}\Omega_e/2)t_{as}}e^{-i(\bar{\omega}_s+\Omega_e/2)t_s}] \tag{5}$$

in which A includes all the constants. Eq. (5) shows that the Rabi oscillation of the two-photon wave packet is produced by the destructive interference of two biphoton channels: Anti-Stokes and Stokes frequencies are either $\bar{\omega}_{as} + \Omega_e/2$, $\bar{\omega}_s - \Omega_e/2$ or $\bar{\omega}_{as} - \Omega_e/2$, $\bar{\omega}_s + \Omega_e/2$, respectively. Therefore, the second-order cross correlation function of Stokes and anti-Stokes is easily obtained as

$$G^{(2)}(\tau) = A'e^{-2\gamma_e\tau}[1 - \cos(\Omega_e\tau)]\Theta(\tau) \tag{6}$$

which clearly shows a oscillation pattern with period $2\pi/\Omega_e$ and damping rate $2\gamma_e$. Balić *et al.* demonstrate the oscillatory behavior with a 3D magneto–optical trap, as shown in Fig. 3.

The group delay condition is $\Omega_e > \Delta\omega_g$ [25, 78], i.e., the two-photon amplitude is determined by the longitudinal detuning function $\Phi(\omega_{as})$, with the third-order
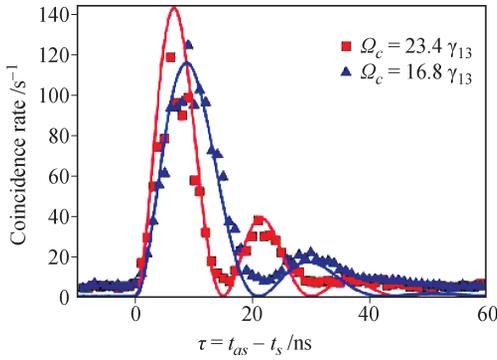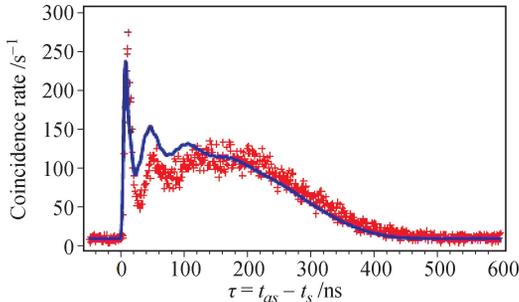
Fig. 3 Coincidence count rate in Rabi oscillation regime. $OD = 11$, $\Omega_p = 0.8\gamma_{13}$, $\Delta\omega_p = 7.5\gamma_{13}$, and $\gamma_{12} = 0.6\gamma_{13}$. The experimental data and theory are shown with diamonds and solid lines, respectively. Reproduced from Ref. [21], Copyright © 2005 American Physical Society.

nonlinear susceptibility treated as a constant. The waveform feature in time domain is thus dominated by the group delay effect. Assuming that the pump laser is weak and far detuned, and the EIT bandwidth $\Delta\omega_{tr} \simeq |\Omega_c|^2/(2\gamma_{13}\sqrt{OD})$ is larger than the phase-matching bandwidth $\Delta\omega_g$, the function $\Phi(\omega_{as})$ is a sinc function, and therefore the two-photon amplitude can be described by a rectangular waveform:

$$\psi(\tau) \simeq \kappa_0 L \tilde{\Phi}(\tau) = \kappa_0 V_g \Pi(\tau; 0, L/V_g) e^{-i\bar{\omega}_{as}\tau} \qquad (7)$$

where κ_0 is the on-resonance nonlinear coupling constant, $\Pi(\tau; 0, L/V_g)$ is the rectangular function ranging from $[0, L/V_g]$. The equal probability of paired photons generation at each space point in the atomic cloud explains the rectangular shape waveform. Moreover, the two-photon correlation time is determined by $\tau_g = L/V_g$, with V_g as the group velocity of anti-Stokes photons. Du *et al.* [25] demonstrated the group delay regime as shown in Fig. 4, with a 2D MOT atom cloud. In this regime, the paired photons are similar with conventional type-II SPDC photons.

Fig. 4 Coincidence count rate in group delay regime. $OD = 30$, $\Omega_p = 1.16\gamma_{13}$, $\Omega_c = 4.2\gamma_{13}$, $\Delta\omega_p = 48.67\gamma_{13}$. The experimental data and theory are shown with diamonds and solid lines, respectively. Reproduced from Ref. [25], Copyright © 2008 American Physical Society.

Other configurations were reported almost simultaneously. Kolchin *et al.* [22] used a single driving laser to serve as the pump and coupling beams. With a stand-

ing wave right angle geometry, they demonstrate paired photons generated within the damped Rabi oscillation regime in a cloud of trapped ^{87}Rb atoms. The biphoton correlation function violates the Cauchy–Schwartz criteria by a factor of 2000. Du *et al.* [28] reported the correlated photons produced from two-level atomic system, in the presence of a retroreflected pump beam. It was the first observation of damped Rabi oscillation in the two-level atomic ensemble, even though the violation of Cauchy–Schwartz inequality was not seen due to Rayleigh scattering. By putting the cold atomic ensemble inside an optical cavity, Thompson *et al.* [63] reported narrowband, identical photon pairs with high-brightness, i.e., high pair generation rates. On the other hand, in hot atomic clouds, SFWM scheme also produces correlated paired photons [64–66].

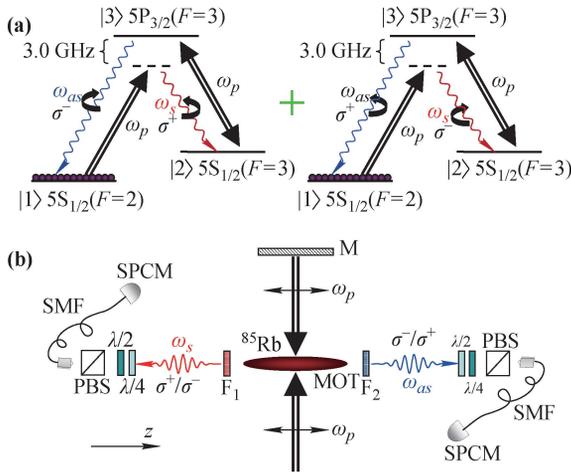### 2.3 Polarization entanglement

In nonlinear crystal, type-I and type-II SPDC are both eligible to produce paired photons with polarization entanglement. As mentioned in Section 1.3, the two-photon wavepackets with polarization states must be indistinguishable in both time and space. On one hand, polarization entanglement can be produced by interfering the photon pair on polarizing beam splitters [16]. On the other hand, entanglement comes from the internal symmetries of the interaction system. In atomic system, polarization entangled states are generated from angular momentum conservation of the four-wave mixing process. Du *et al.* [24] suggested and discussed the possibility of paired photon with polarization entanglement generated in a three-state system of cold atomic ensemble.

Yan *et al.* [79] demonstrated experimentally the scheme to generate the hyperentangled narrow-band paired photons. Figure 5 shows the relevant ^{85}Rb D2 line energy level diagram and the experimental configuration. The strong, linearly polarized pump beam is applied onto the 2D MOT transversely and retro-reflected by a mirror. The pump laser acts not only as the pump beams of the SFWM process but also as the coupling beam of the EIT process for anti-Stokes photons. Obviously, the paired photons produced from this scheme are nondegenerate and their central optical frequencies differ by 6 GHz, i.e., $\omega_{as0} - \omega_{s0} = 2\Delta_{12}$. The optical filter at each side distinguish Stokes and anti-Stokes photons spatially. The time-frequency entanglement between the Stokes and anti-Stokes photons is preserved in the right-angle configuration. On the other hand, the entanglement in polarization is enabled by the degenerate Zeeman sub states of each hyperfine energy level. By choosing the 2D MOT longitudinal symmetry axis as the quantization z axis, Zeeman states with $\Delta M_F = 0$ are coupled by the linearly polarized pump beams and thus

$\Delta M_{\rm F} = 0$ transitions are excited mostly. Conservation of angular momentum along the z axis allows two possible circular polarization configurations as shown in Fig. 5(a). Therefore the hyperentangled quantum state of the paired Stokes and anti-Stokes photons are described by

$$| \Psi_{s,as}(t_s, t_{as}) \rangle = \psi(\tau) {\rm e}^{-{\rm i}\bar{\omega}_s t_s} {\rm e}^{-{\rm i}\bar{\omega}_{as} t_{as}}$$
$$\times \frac{1}{\sqrt{2}} (|\sigma_s^+ \sigma_{as}^- \rangle + |\sigma_s^- \sigma_{as}^+ \rangle)) \quad (8)$$

where the two-photon amplitude in time domain is $\psi(\tau)$, which include the time-frequency entanglement properties of paired photon generated.

Fig. 5 Schematics of narrowband nondegenerate hyperentangled paired photon generation. **(a)** ^{85}Rb energy level diagram with two possible polarization configurations for the spontaneously emitted photon pairs. **(b)** Experimental setup with right-angle geometry. Reproduced from Ref. [79], Copyright © 2011 American Physical Society.

Concerning the polarization entanglement, the density matrix of the paired photons polarization state is determined from quantum-state tomography measurement. The graphical representation for the density matrix is shown in Fig. 6. The result shows a fidelity of 90.8% between the measured state and the ideal EPR-Bell state. From time-domain coincidence measurement, these narrow-band hyperentangled photons have coherence time of about 30 ns, and are suitable for quantum-memory based long distance quantum communication [79].
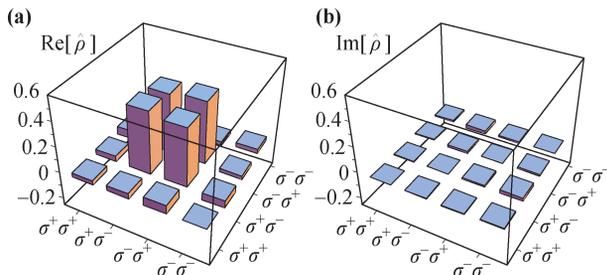
Fig. 6 Tomography measurement result of the polarization-entangled paired photons: **(a)** Real parts and **(b)** imaginary parts of the density matrix.

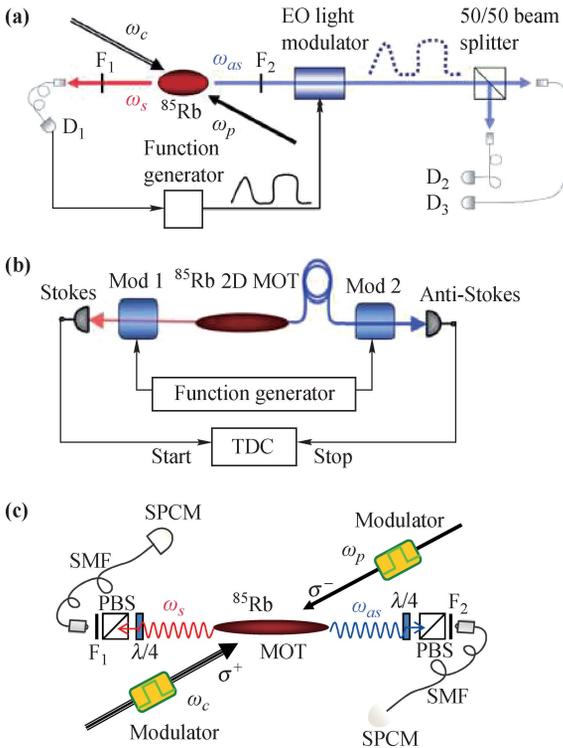## 3 Narrowband paired photons waveform reshaping

Appropriate spectral manipulation change the joint bandwidth of the paired photons generated in SPDC. Generally speaking, the length or the dispersive properties of the nonlinear crystal, the spectral or the spatial properties of the pump beam are all available factors that manipulate the bandwidth and therefore the temporal correlations of the SPDC paired photons. By applying the coherent pulse-shaping techniques onto the entangled paired photons generated from down-converting crystal, Pe'er *et al.* [80] demonstrated the spectral-phase manipulations to the paired photons actually reshape the two-photon temporal wave function. With four prisms arranged after the down-converted crystal, the spectral information of the paired photons converted to a spectral Fourier plane, through which a computer-controlled spatial light modulator manipulated the spectral-phase properties of the entangled photons. Viciani *et al.* [81] experimentally and theoretically demonstrated another spectral or temporal shaping by using a monochromator or air-spaced etalons on the idler path. Hendrych *et al.* [82] employed the angular dispersion to modify the spatial distribution of the pump beam and the phase mismatching Δ_k of the joint spectrum of paired photons. On the other hand, by modulating the spatial mode of the pump beam, Valencia *et al.* [84] transferred the spatial information of the pump field into the joint spectrum of the SPDC photons.

Quasi-phase matching technique developed quickly as an efficient method to reshape paired photon source. Carrasco *et al.* [83] theoretically introduced a chirped quasi-phase matching (QPM) nonlinear crystal structure to broaden the spectral width of the generated paired photons. The crystal is designed in such a way that the phase-matching conditions vary longitudinally by use of QPM with a chirped period. On this basis, Harris [85] further introduced QPM as an efficient way for pulse reshaping toward single-cycle biphotons. Nasr *et al.* [87] utilized ultranarrow Hong–Ou–Mandel dip measurement to characterize the ultra-short correlation time of paired photons generated from chirped QPM. With Sum frequency generation (SFG), Sensarn *et al.* [86] measured the amplitude of the paired photon wave function, and demonstrated that temporal width compression of a factor of 5 is achieved.

Nonlocal modulation, the time–frequency analog to nonlocal dispersion cancellation [88], is an important consequence of time–energy entanglement. Phase modulation in idler channel can act cumulatively with modulation in signal channel, no matter how distantly the two modulators separate. Nonlocal modulation has been firstly observed [89, 90] with SPDC paired photons.

Paired photons generated in write–read process, where signal photon delay is programmable, cannot be applied with nonlocal modulation.

Paired photon produced from conventional spontaneous parametric down-conversion is difficult to be manipulated in time, mainly due to their wide bandwidth (∼THz) and short coherence time (∼ps). Therefore, access to paired photons with controllable time–space waveforms is limited in SPDC literature. Narrowband paired photons generated in atomic ensembles via FWM with long coherence time (0.1–1 µs) enable measurement over their temporal waveform directly using commercial detectors. By passing these long single photons through electro–optical modulators, it is possible to modulate one of the paired photons [91] or their correlation function [92], as Figs. 7(a) and (b) show.


Fig. 7 Schematics of narrowband paired photons temporal waveform modulation and reshaping. Three schemes include: **(a)** Modulation on the anti-Stokes photons, **(b)** Synchronous modulation on the paired photons, **(c)** Modulation on the classical controll beams.

Kolchin *et al.* [91] demonstrated the use of one photon of a photon pair to establish the time origin for the modulation of the second one, as shown in Fig. 7(a). Using an EO-modulator inserted in the path of anti-Stokes light beam, the photon waveform may be modulated in the same manner as a classical light pulse, once the time origin is established. With this scheme, reshaping of the single photon waveform become straightforward. The conditional single-photon wave packet can be described by

$$\psi_0(\tau) = \langle 0|m(\tau)\hat{a}_{as}(t_s + \tau)\hat{a}_s(t_s)|\Psi_{s,as}\rangle|_{t_s=0}$$

$$= \frac{1}{2\pi} \int \Phi_0(\omega) e^{-i\omega\tau} d\omega \tag{9}$$

where $m(\tau)$ is the amplitude modulation function as the relative time delay. Figure 8 shows the reshaped biphoton waveform via this scheme. A measure of the quality of heralded single photons is given by the conditional auto-correlation function $g_c^{(2)} = N_{123}N_1/N_{12}N_{13}$ [93]. The measured $g_c^{(2)}$ is less than 0.5 (the limiting value for a two-photon Fock state), and therefore the near-single-photon character of the photons was satisfactory.
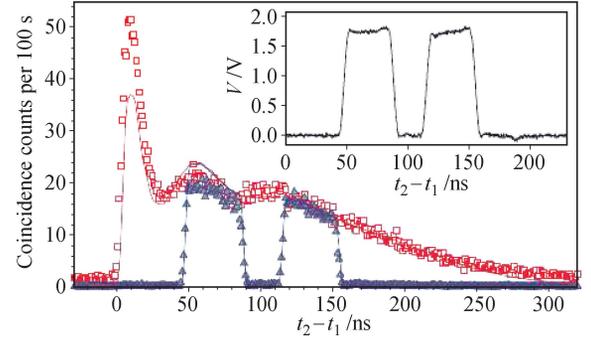
Fig. 8 Coincidence counts in a 1 ns bin as a function of time delay τ, with anti-Stokes beam modulated by an EO-modulator. △ denote modulated waveform and □ denote unmodulated waveform. Reproduced from Ref. [91], Copyright ⓒ 2008 American Physical Society.

Belthangady *et al.* [92] described a proof-of-principle experiment for modulation with amplitude EO-modulators inserted into both paired photon light beams. Figure 7(b) shows their modulation scheme. Stokes and anti-Stokes photons are modulated by two amplitude modulators which are controlled by the same function generator with two output channels with arbitrary phase difference. If the detectors are slow in the sense that the coincidence counts is integrated over the delay time τ, one obtains the Fourier cosine transform pair for the coincidence counts.

For both modulation methods, these external modulators are directly applied on the anti-Stokes field for reshaping, and thus a large number of single photons are wasted in the photon attenuation. Moreover, in these experiments where amplitude modulation is performed using Mach–Zehnder interferometers, coupling between the single photons and the environment at the beam splitters introduces noises (uncorrelated photons) into the system. Following the theoretical work by Du *et al.* [94], Chen *et al.* [95] experimentally demonstrated the shaping of the temporal quantum waveform of narrow-band biphotons, by periodically modulating the two driving fields in the FWM process, as shown in Fig. 7(c). The input field profiles can be thus mapped into the two-photon waveform with arbitrarily shaped correlation function. The principle of this modulation method is an temporal analog of the spatial modulation technique reported by Monken *et al.* [96], in which they demonstrated that the angular

spectrum of the pump beam can be transferred to the paired photon transverse correlation.

The physical picture is simple. The periodically modulated pump and coupling laser fields are decomposed in frequency domain into discrete frequency components. As a result, paired photon generation follows many possible FWM paths. The interference between these multichannel FWMs provides a controllable way to manipulate and engineer the paired photon wave packets. Usually, the near-atomic-resonance nonlinear process with time varying pump and coupling lasers is not solved analytically. However, when the atomic optical depth in the transition $|1\rangle \to |3\rangle$ is high and the EIT slow-light effect is significant, the theoretical analysis becomes greatly simplified. In this case, $\kappa(\omega_{as})$ can be considered a constant. With weak pump excitation, ground-state approximation is appropriate and thus the frequency dispersion of the Stokes photon can be ignored. It means that we can treat all the Stokes photons traveling with the speed of light in vacuum. The anti-Stokes fields are experiencing EIT slow light effect. If the frequency modulation to coupling laser is small enough (< 10 MHz), we could assume that the multiple EIT channels are equivalent. Therefore the group velocities associated with different anti-Stokes channels (denoted by m channels) are the same and can be considered to be controlled by the average intensity of the coupling beam, i.e., $V_{gm} = V_g \ll c$. The time-averaged correlation becomes

$$\bar{R}(\tau) = C(\tau)R_0(\tau) \tag{10}$$

where $C(\tau) \equiv \lim_{\Delta T \to 0} \frac{1}{\Delta T I_p I_c} \int_0^{\Delta T} \bar{I}_p(t)\bar{I}_c(t + \tau)\mathrm{d}t$ is the time-averaged pump-coupling correlation function. $R_0(\tau)$ is the correlation function without modulation. The scheme is not limited to identical modulations. By modulating the pump and coupling with different waveforms, it is possible to generate correlation with arbitrary waveforms. In particular, if the pump laser is modulated by short Gaussian pulses (equivalent to a δ function), and the coupling laser is modulated by a square followed by a triangle shape with the same modulation period, we expect to obtain a correlation function with the shape of the modulation waveform imposed on the coupling laser. Figure 9 shows the reshaped waveform.

4   Conclusions and outlook

We review the experimental works on narrow-band paired photons generated via SFWM processes in atomic ensembles. With continuous controlling fields, we are able to produce time–frequency entangled paired photons. They are easy to be modulated directly in time domain and thus be reshaped. The photon pairs are nonclassical light sources, which dramatically violate the Cauchy–Schwartz inequality. Also, this type of paired
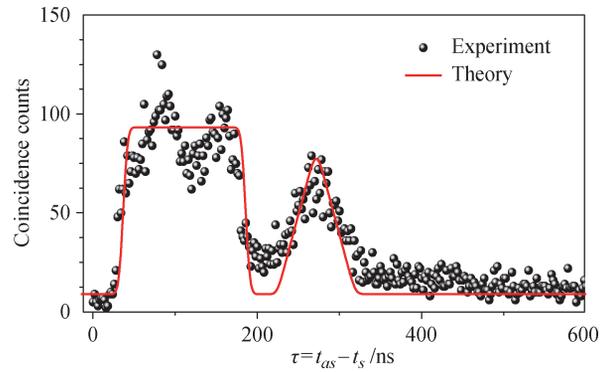
Fig. 9 Two-photon correlation function with nonidentical modulations on the pump and coupling lasers. Reproduced from Ref. [95], Copyright © 2010 American Physical Society.

photons are potential to be entangled in more than two dimensions.

Correlated paired photons give birth to heralded single photon, with one of the paired photons serving the flag to announce the other one. In quantum network and communication, single photon state is more preferable [67–70]. A single photon is described by Fock-state in quantum mechanics. The propagation of a single photon was investigated only in a few and limited experiments [68, 71]. One major reason is that the single photon wave function is beyond manipulation. The progress in generating narrowband paired photons with controllable waveform facilitates the experimental setup to verify such a problem. The waveform of the heralded single photon is shaped by electro–optical modulator (EOM) [72–74], and thus arbitrary waveform can be generated. Optical precursor of a single photon is observed with single photon waveform reshaped to having sharp rising or falling edges [97]. This is the first experimental direct evidence for the speed limit of a single photon, i.e., a single photon would propagate through medium with the limit of the speed of light in vacuum c. Further, fundamental topics concerning traditional optical phenomena including free-induction decay can be explored with single photon level. On the other hand, quantum key distribution, which calls for narrow-band single photon source, also benefits from the development of narrow-band paired photons [98].

References

1. S. L. Braunstein and P. van Loock, Rev. Mod. Phys., 2005, 77(2): 513

2. N. Gisin, G. Ribordy, W. Tittel, and H. Zbinden, Rev. Mod. Phys., 2002, 74(1): 145

3. M. D'Angelo and Y. H. Shih, Laser Phys. Lett., 2005, 2: 567

4. C. S. Wu and I. Shaknov, Phys. Rev., 1950, 77(1): 136

5. C. A. Kocher and E. D. Commins, Phys. Rev. Lett., 1967, 18(15): 575

6. A. Aspect, P. Grangier, and G. Roger, Phys. Rev. Lett., 1981, 47(7): 460

7. S. E. Harris, M. K. Oshman, and R. L. Byer, Phys. Rev. Lett., 1967, 18(18): 732

8. D. Burnham and D. Weinberg, Phys. Rev. Lett., 1970, 25(2): 84

9. M. H. Rubin, D. N. Klyshko, Y. H. Shih, and A. V. Sergienko, Phys. Rev. A, 1994, 50(6): 5122

10. Y. H. Shih, Rep. Prog. Phys., 2003, 66(6): 1009

11. D. N. Klyshko, Photons and Nonlinear Optics, Gordon and Breach, 1998

12. Z. Y. Ou and Y. J. Lu, Phys. Rev. Lett., 1999, 83(13): 2556

13. H. Wang, T. Horikiri, and T. Kobayashi, Phys. Rev. A, 2004, 70(4): 043804

14. C. E. Kuklewicz, F. N. C. Wong, and J. H. Shapiro, Phys. Rev. Lett., 2006, 97(22): 223601

15. J. S. Neergaard-Nielsen, B. M. Nielsen, H. Takahashi, A. I. Vistnes, and E. S. Polzik, Opt. Express, 2007, 15(13): 7940

16. X.-H. Bao, Y. Qian, J. Yang, H. Zhang, Z.-B. Chen, T. Yang, and J.-W. Pan, Phys. Rev. Lett., 2008, 101(19): 190501

17. F.-Y. Wang, B.-S. Shi, and G.-C. Guo, Opt. Lett., 2008, 33(19): 2191

18. L. M. Duan, M. D. Lukin, J. I. Cirac, and P. Zoller, Nature, 2001, 414(6862): 413

19. C. H. van der Wal, M. D. Eisaman, A. André, R. L. Walsworth, D. F. Phillips, A. S. Zibrov, and M. D. Lukin, Science, 2003, 301(5630): 196

20. A. Kuzmich, W. P. Bowen, A. D. Boozer, A. Boca, C. W. Chou, L. M. Duan, and H. J. Kimble, Nature, 2003, 423(6941): 731

21. V. Balić, D. A. Braje, P. Kolchin, G. Y. Yin, and S. E. Harris, Phys. Rev. Lett., 2005, 94(18): 183601

22. P. Kolchin, S. Du, C. Belthangady, G. Y. Yin, and S. E. Harris, Phys. Rev. Lett., 2006, 97(11): 113602

23. J. M. Wen, S. Du, and M. H. Rubin, Phys. Rev. A, 2007, 76: 013825

24. S. Du, E. Oh, J. Wen, and M. H. Rubin, Phys. Rev. A, 2007, 76(1): 013803

25. S. Du, P. Kolchin, C. Belthangady, G. Y. Yin, and S. E. Harris, Phys. Rev. Lett., 2008, 100(18): 183603

26. X.-S. Lu, Q.-F. Chen, B.-S. Shi, and G.-C. Guo, Chin. Phys. Lett., 2009, 26(7): 064204

27. P. Chen, S.-Y. Zhou, Z. Xu, Y.-F. Duan, G.-D. Cui, T. Hong, and Y.-Z. Wang, Chin. Phys. Lett., 2011, 28(7): 074214

28. S. Du, J. Wen, M. H. Rubin, and G. Y. Yin, Phys. Rev. Lett., 2007, 98(5): 053601

29. T. W. Hänsch and A. L. Schawlow, Opt. Commun., 1975, 13: 68

30. S. Chu, L. Hollberg, J. E. Bjorkholm, A. Cable, and A. Ashkin, Phys. Rev. Lett., 1985, 55(1): 48

31. E. L. Raab, M. Prentiss, A. Cable, S. Chu, and D. E. Pritchard, Phys. Rev. Lett., 1987, 59(23): 2631

32. P. D. Lett, R. N. Watts, C. I. Westbrook, W. D. Phillips, P. L. Gould, and H. J. Metcalf, Phys. Rev. Lett., 1988, 61(2): 169

33. S. E. Harris, Phys. Today, 1997, 50(7): 36

34. M. Fleischhauer, A. Imamoglu, and J. P. Manarangos, Rev. Mod. Phys., 2005, 77(2): 633

35. U. Volz and H. Schmoranzer, Physica Scripta, 1996, T65: 48

36. J. E. Simsarian, L. A. Orozco, G. D. Sprouse, and W. Z. Zhao, Phys. Rev. A, 1998, 57(4): 2448

37. S. E. Harris and L. V. Hau, Phys. Rev. Lett., 1999, 82(23): 4611

38. D. A. Braje, V. Balić, G. Y. Yin, and S. E. Harris, Phys. Rev. A, 2003, 68(4): 041801(R)

39. P. Grangier, G. Roger, A. Aspect, A. Heidmann, and S. Reynaud, Phys. Rev. Lett., 1986, 57(6): 687

40. A. Heidmann and S. Reynaud, J. Mod. Opt., 1987, 34(6–7): 923

41. A. Aspect, G. Roger, S. Reynaud, J. Dalibard, and C. Cohen-Tannoudji, Phys. Rev. Lett., 1980, 45(8): 617

42. M. W. Mitchell, C. I. Hancox, and R. Y. Chiao, Phys. Rev. A, 2000, 62(4): 043819

43. A. Einstein, B. Podolsky, and N. Rosen, Phys. Rev., 1935, 47(10): 777

44. J. S. Bell, Physics, 1964, 1: 195

45. J. F. Clauser, M. A. Horne, A. Shimony, and R. A. Holt, Phys. Rev. Lett., 1969, 23(15): 880

46. J. C. Howell, R. S. Bennink, S. J. Bentley, and R. W. Boyd, Phys. Rev. Lett., 2004, 92(21): 210403

47. D. N. Matsukevich and A. Kuzmich, Science, 2004, 306(5696): 663

48. P. G. Kwiat, K. Mattle, H. Weinfurter, A. Zeilinger, A. V. Sergienko, and Y. Shih, Phys. Rev. Lett., 1995, 75(24): 4337

49. Y. H. Shih and C. O. Alley, Phys. Rev. Lett., 1988, 61(26): 2921

50. Y. H. Shih, A. V. Sergienko, and H. Morton, Phys. Rev. A, 1994, 50(1): 23

51. C. K. Law, I. A. Walmsley, and J. H. Eberly, Phys. Rev. Lett., 2000, 84(23): 5304

52. M. N. O'Sullivan-Hale, I. Ali Khan, R. W. Boyd, and J. C. Howell, Phys. Rev. Lett., 2005, 94: 220501

53. I. A. Khan and J. C. Howell, Phys. Rev. A, 2006, 73: 031801(R)

54. B.-S. Shi, C. Zhai, F.-Y. Wang, and G.-C. Guo, Front. Phys. China, 2010, 5(2): 131

55. C. S. Chuu and S. E. Harris, Phys. Rev. A, 2011, 83(6): 061803(R)

56. R. H. Stolen, J. E. Bjorkholm, and A. Ashkin, Appl. Phys. Lett., 1974, 24(7): 308

57. K. O. Hill, D. C. Johnson, B. S. Kawasaki, and R. I. MacDonald, J. Appl. Phys., 1978, 49(10): 5098

58. K. Washio, D. Inoue, and S. Kishida, Electron. Lett., 1980, 16(17): 658

59. C. L. Lin, W. A. Reed, A. D. Pearson, and H. T. Shang, Opt. Lett., 1981, 6(10): 493

60. K. Tai, A. Hasegawa, and A. Tomita, Phys. Rev. Lett., 1986, 56(2): 135

61. T. A. B. Kennedy, Phys. Rev. A, 1991, 44(3): 2113

62. L. J. Wang, C. K. Hong, and S. R. Friberg, J. Opt. B, 2001, 3(5): 346

63. J. K. Thompson, J. Simon, H. Loh, and V. Vuletić, Science, 2006, 313(5783): 74

64. Q. F. Chen, B.-S. Shi, M. Feng, Y.-S. Zhang, and G.-C. Guo, Opt. Express, 2008, 16(26): 21708

65. R. T. Willis, F. E. Becerra, L. A. Orozco, and S. L. Rolston, Phys. Rev. A, 2010, 82(5): 053842

66. D.-S. Ding, Z.-Y. Zhou, B.-S. Shi, X.-B. Zou, and G.-C. Guo, Opt. Express, 2012, 20: 11433

67. D. N. Matsukevich and A. Kuzmich, Science, 2004, 306(5696): 663

68. M. D. Eisaman, A. André, F. Massou, M. Fleischhauer, A. S. Zibrov, and M. D. Lukin, Nature, 2005, 438(7069): 837

69. T. Chanelière, D. N. Matsukevich, S. D. Jenkins, S. Y. Lan, T. A. B. Kennedy, and A. Kuzmich, Nature, 2005, 438(7069): 833

70. A. G. Radnaev, Y. O. Dudin, R. Zhao, H. H. Jen, S. D. Jenkins, A. Kuzmich, and T. A. B. Kennedy, Nat. Phys., 2010, 6(11): 894

71. A. M. Steinberg, P. G. Kwiat, and R. Y. Chiao, Phys. Rev. Lett., 1993, 71(5): 708

72. P. Kolchin, C. Belthangady, S. Du, G. Y. Yin, and S. E. Harris, Phys. Rev. Lett., 2008, 101(10): 103601

73. C. Belthangady, S. Du, C. S. Chuu, G. Y. Yin, and S. E. Harris, Phys. Rev. A, 2009, 80(3): 031803(R)

74. J. F. Chen, S. Zhang, H. Yan, M. M. T. Loy, G. K. L. Wong, and S. Du, Phys. Rev. Lett., 2010, 104(18): 183604

75. P. Kolchin, Phys. Rev. A, 2007, 75(3): 033814

76. J. Wen and M. H. Rubin, Phys. Rev. A, 2006, 74(2): 023808

77. J. Wen and M. H. Rubin, Phys. Rev. A, 2006, 74(2): 023809

78. S. Du, J. M. Wen, and M. H. Rubin, J. Opt. Soc. Am. B, 2008, 25(12): C98

79. H. Yan, S. Zhang, J. F. Chen, M. M. T. Loy, G. K. L. Wong, and S. Du, Phys. Rev. Lett., 2011, 106(3): 033601

80. A. Pe'er, B. Dayan, A. A. Friesem, and Y. Silberberg, Phys. Rev. Lett., 2005, 94(7): 073601

81. S. Viciani, A. Zavatta, and M. Bellini, Phys. Rev. A, 2004, 69(5): 053801

82. M. Hendrych, X. Shi, A. Valencia, and J. P. Torres, Phys. Rev. A, 2009, 79(2): 023817

83. S. Carrasco, J. P. Torres, L. Torner, A. Sergienko, B. E. Saleh, and M. C. Teich, Opt. Lett., 2004, 29(20): 2429

84. A. Valencia, A. Ceré, X. Shi, G. Molina-Terriza, and J. P. Torres, Phys. Rev. Lett., 2007, 99(24): 243601

85. S. E. Harris, Phys. Rev. Lett., 2007, 98(6): 063602

86. S. Sensarn, G. Y. Yin, and S. E. Harris, Phys. Rev. Lett., 2010, 104(25): 253602

87. M. B. Nasr, S. Carrasco, B. E. A. Saleh, A. V. Sergienko, M. Teich, J. Torres, L. Torner, D. Hum, and M. Fejer, Phys. Rev. Lett., 2008, 100(18): 183601

88. J. D. Franson, Phys. Rev. A, 1992, 45(5): 3126

89. S. E. Harris, Phys. Rev. A, 2008, 78(2): 021807(R)

90. S. Sensarn, G. Y. Yin, and S. E. Harris, Phys. Rev. Lett., 2009, 103(16): 163601

91. P. Kolchin, C. Belthangady, S. Du, G. Y. Yin, and S. E. Harris, Phys. Rev. Lett., 2008, 101(10): 103601

92. C. Belthangady, S. Du, C. S. Chuu, G. Y. Yin, and S. E. Harris, Phys. Rev. A, 2009, 80(3): 031803(R)

93. P. Grangier, G. Roger, and A. Aspect, Europhys. Lett., 1986, 1(4): 173

94. S. Du, J. M. Wen, and C. Belthangady, Phys. Rev. A, 2009, 79(4): 043811

95. J. F. Chen, S. Zhang, H. Yan, M. M. T. Loy, G. K. L. Wong, and S. Du, Phys. Rev. Lett., 2010, 104(18): 183604

96. C. H. Monken, P. H. Souto Ribeiro, and S. Pádua, Phys. Rev. A, 1998, 57(4): 3123

97. S. Zhang, J. F. Chen, C. Liu, M. M. T. Loy, G. K. L. Wong, and S. Du, Phys. Rev. Lett., 2011, 106(24): 243602

98. H. Yan, S. L. Zhu, and S. Du, Chin. Phys. Lett., 2011, 28(7): 070307